Journal of Medicinal and Chemical Sciences 6 (2023) 1193-1203

Journal of Medicinal and Chemical Sciences

Journal homepage: http://www.jmchemsci.com/

Original Article

Cilostazol Protects Against Sepsis-Induced Kidney Impairment in a Mice Model

Abdulla K Raheem[1,*], Ahmed R. Abu-Raghif[2], Qassim A Zigam[3]

[1]*Pharmacy Department, Al-Mustaqbal University College, Babylon, Iraq*
[2]*Department of Pharmacology, College of Medicine, Al-Nahrain University, Baghdad, Iraq*
[3]*Pharmacy Department, Al-Mustaqbal University College, Babylon, Iraq*

ARTICLE INFO

Article history

Receive: 2022-07-08
Received in revised: 2022-08-23
Accepted: 2022-11-01
Manuscript ID: JMCS-2210-1797
Checked for Plagiarism: **Yes**
Language Editor:
Dr. Nadereh Shirvani
Editor who approved publication:
Professor Dr. Ehab AlShamaileh

DOI:10.26655/JMCHEMSCI.2023.5.25

KEYWORDS

CLP
Polymicrobial sepsis
Renal injury
NGAL
Oxidative stress

ABSTRACT

Sepsis is a type of systemic inflammatory disease caused by polymicrobial infection. To investigate the potential reno-protective benefits of cilostazol during sepsis-induced renal injury, forty male albino Swiss mice, 25 to 30 grams in weight and 8 to 12 weeks old, were employed in the present investigation. Both food and water were freely available to these animals. Mice were separated into the following four groups after two weeks of adaption. (n = 10): (1) Healthy group: apparently normal mice. (2) induced group: mice underwent cecal ligation and puncture operation. (3) DMSO group: mice received DMSO as a vehicle (4) cilostazol group: Cilostazol was administered intraperitoneally to mice for five days in a row at a dose of 5 mg/kg/day. Compared to the CLP group, the cilostazol group showed a significantly ($p<0.05$) lower amount of NGAL in the kidneys. Additionally, compared to the CLP group, the cilostazol group showed a substantial ($p0.05$) decline in the levels of serum of inflammatory cytokines (IL-1β, TNF-α, & Interleukin-6). Additionally, compared to the CLP group, the cilostazol group had a significantly ($p<0.05$) increased renal SOD activity and decreased MDA level. Histologically, all animals in the CLP group displayed a substantial level of kidney tissue damage ($p<0.05$), whereas the cilostazol group displayed a significantly diminished level of kidney tissue injury. Their capacity to lower serum levels of pro-inflammatory cytokines (IL-1β, TNF-α, and IL-6) has an anti-inflammatory impact. Additionally, they have an antioxidant impact by raising renal SOD activity and lowering renal MDA levels.

GRAPHICAL ABSTRACT

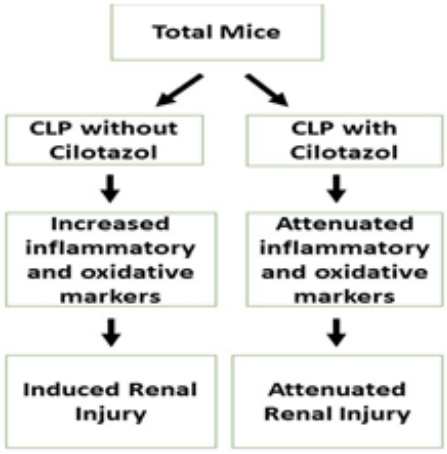

* Corresponding author: Abdulla K Raheem
✉ E-mail: Email: abdullaalkhakani76@yahoo.com

Introduction

Sepsis is a serious public health issue across the world, with an increased mortality rate. The Intensive Care Over Nations (ICON) research was collected worldwide. According to epidemiologic studies on 10,069 intensive-care unit (ICU) patients, 2,973 (29.5%) had sepsis at arrival or during their stay. ICU mortality rates for patients with sepsis were 25.8%, while hospital mortality rates were 35.3%, significantly higher than the ICU mortality rate for all patients. Evidence-based sepsis management is necessary to reduce mortality, as the Surviving Sepsis Program has shown over the past ten years [1]. Sepsis, characterized by life-threatening organ failure, results from an unbalanced host response to infection. Suspected or confirmed infection and a sharp rise in two or more consecutive organ failure assessments' (SOFA) values used as a proxy for actual organ failure are the clinical criteria for sepsis. A type of sepsis called septic shock occurs when the underlying metabolic and circulatory problems are so severe that the risk of death is greatly increased. Despite sufficient fluid resuscitation, the clinical sepsis criteria define septic shock.

Moreover, a vasopressor needs to achieve lactate >2mmol/L (18 mg/dl) and mean arterial pressure >65 mm Hg. Compared to the death rate related to the original definition of sepsis, which was 10%, The revised septic shock criteria are associated with a high fatality rate (40%) [2]. When blood cultures are positive, AKI appears in roughly 19% of people with mild sepsis, 23% with severe sepsis, and 51% with septic shock. The beginning and ending supportive therapy (BEST) kidney investigators discovered that sepsis was the most frequent cause of AKI in critically sick patients after assessing a broad community in 54 hospitals spread across 23 different nations (47.5 percent). They concluded that septic AKI was linked to more abnormal hemodynamic and biochemical indicators, worse disease severity, and a higher requirement for mechanical ventilation and vasopressor treatment. This research revealed a few additional facts. In septic AKI, oliguria was more prevalent (67 percent vs. 57 percent; P 0.001). Compared to nonseptic AKI, Septic AKI had a greater rate of in-hospital fatalities (70.2 vs. 51.8 percent; p 0.001). The median ICU and hospital stays length was greater for survivors of septic AKI (37 vs. 21d; P 0.0001) [3]. In critically ill patients, The most frequent reason for AKI is sepsis. Despite this, the pathophysiological processes of S-AKI remain unknown. As a result, treatment is reactive and vague, and no preventative therapies are available [4]. Hypoperfusion and shock are associated with the major causes of AKI (such as sepsis, surgical intervention, heart failure, and hypovolemia), and ischemia damage can result in significant cell harm (e.g., severe tubular necrosis). However, it is becoming evident that other mechanisms must work and that ischemia-reperfusion damage is not the primary mechanism generating S-AKI [5].

Cilostazol is a quinolone precursor principally used to relieve intermittent claudication caused by the early stages of peripheral vascular disease. A disease called intermittent claudication is brought on when the arteries that supply the legs with oxygen narrow [6].

PDE3 (phosphodiesterase III) is inhibited by cilostazol. Cyclic guanosine monophosphate and cyclic adenosine monophosphate (cAMP) are hydrolyzed by the catalytic core of PDE3 enzymes (cGMP). Phosphodiesterase III enzymes regulate the contractility of cardiac and vascular smooth muscle in the sarcoplasmic reticulum of the heart and the smooth muscle of the veins and arteries [7].

Cilostazol works by lowering phosphodiesterase activity and limiting cAMP breakdown. Platelets and blood arteries can produce more cAMP thanks to PDE3 inhibition. Higher cAMP levels result in a more concentrated active form of protein kinase A (PKA), and higher PKA levels are directly related to the prevention of platelet aggregation [8].

Investigate the anti-inflammatory properties and anti-oxidant effects of cilostazol in sepsis and also assess the effect of cilostazol on the renal histopathological outcomes in the experimental model

Material and Methods

Chemical and drugs

We acquired cilostazol powder from Beijing Cooperate Pharm, China. Prepared in a diluted DMSO vehicle [9]. Cilostazol was given intraperitoneally in a once-daily dose of 5 mg/kg/day [10, 11].

Animals of THE study

In the current investigation, 40 male mice between the ages of 8 and 12 weeks weighing 25 to 30 g were employed. These mice were placed in cages in an animal home with 12:12 light: dark cycles, a room temperature of 25 °C, a humidity level of 60–65%, and free access to food and drink.

Design of the study

After giving the forty mice two weeks to acclimate, they were divided into the following groups, each with ten mice:

1. Normal group: Apparently healthy animals.
2. Septic group: The induction procedure was conducted without treatment.
3. Vehicle group: The same volume of DMSO was administered intraperitoneally to the mice in this group.
4. Cilastazol group: For five days, animals in this group received Cilastazol 5 mg/kg/day intraperitoneally, and on the fourth day, CLP started working [11].

The experimental model of sepsis induction (CLP)

In the current study, mice were used to develop polymicrobial sepsis. Based on previous research, The CLP (cecal ligation and puncture) paradigm was used to create sepsis [12, 13]. In brief, During the first 24 hours of sepsis, the two-puncture method was combined with an 18-g needle to cause organ (renal) dysfunction. The Mice were anesthetized with a mixture of anesthetic solution that involved xylazine (20 mg/mL) and ketamine (100 mg/mL) in a1: 2 combination ratio [14]. Following that, the mouse's abdomen was given the cecum was exposed after a 2 cm midline incision. After ligating and puncturing the cecum right below the ileocecal valve, the cecum was relocated anatomically. To check the integrity of the puncture sites, a tiny sample of stool was removed. After that, the abdomen was sutured. Then, normal saline (20 mL/kg body weight) was administered subcutaneously to the animals as a resuscitative dose.

Samples collection

Aft the anesthesia-induced sacrifice of the mice on the fifth day, tissue and blood samples were collected in the manner described below:

Blood sampling

Using the direct heart puncture approach, blood was drawn after the scarification surgery. The clotting process was allowed to occur by centrifuging the blood after it had been drawn for about 10 minutes at 10,000 rpm. The supernatant was then stored at -20 °C for further analysis.

Renal homogenization

Renal tissue was removed and divided into two halves after the experiment. After being cleansed with saline to eliminate any red blood cells or clots, one piece of kidney tissue was mashed in a 1:10 (w/v) phosphate-buffered saline (pH 7.4) solution having a protease inhibitor cocktail and 1% Triton X-100 [15]. High-intensity use of a liquid processor. Samples were homogenized and spun at 10,000 rpm for 20 minutes at 4 °C [16]. The supernatant was then gathered and utilized to quantify NGAL, MDA, and SOD. The other renal portion was examined histopathologically.

Outcome measurement

Inflammatory cytokines including (IL-1β, IL-6, and TNF-α)

The serum concentrations of IL-1β, IL-6, and TNF-α were assessed using an ELISA in accordance with the manufacturer's instructions. Mouse IL-1β, IL-6, and TNF-α antibodies had been pre-coated on the ELISA kit plate. The samples' IL-1β, IL-6, and TNF-α levels were increased, then bound to antibodies and coated on the wells. Then, Mouse IL-1β, IL-6, and TNF-α antibodies that had been biotinylated were introduced and bound to the samples' IL-1β, TNF-

α, and IL-6 levels. The biotinylated IL-1β, IL-6, and TNF-α antibodies were combined with streptavidin-HRP and bound. After incubation, unbound Streptavidin-HRP has washed away through a washing process. Subsequently, after adding the substrate solution, the amount of Mouse IL-1β, IL-6, and TNF-α affected how the color changed. At 450 nm, Measurements of absorbance were made after the process was stopped by adding an acidic stop solution.

ELISA measurement of serum ngal

Fill the appropriate wells with 100 µl of each standard and sample. With a gentle shake, cover tightly and 90 minutes duration of the incubation period at ambient temperature or overnight at 4 °C. The lid should be taken off, the solution discarded, and the plate should be washed three times with the Wash Buffer Working Solution, letting the solution sit in the wells between washes for a minute or two. Place paper towels or another absorbent material nearby to blot the plate. The wells should never be allowed to dry or fill each well with 100 µl of the Biotin-Labeled Identification Antibody Working Solution, and incubate the plate for 60 minutes at 37°C. Wash the plate with Wash Buffer Working Solution three times; give each application a 1-2 minute window of time in the wells. Use a towel or another insulating material to blot the dish after washing it with a buffer solution and throwing it away. The plate was incubated at 37 °C for 45 minutes after each well had added 100 µl of the streptavidin-HRP working solution. With Elution Buffer Working Solution, rinse the plate five times, allowing the wash buffer to remain in each well for one to two minutes. Throw away the elution buffer and blot the dish with a towel or other insulating material. 100 µl of TMB Substrate Solution should be added to each well before the plate is incubated at 37 °C in the dark for 30 minutes.

Oxidative stress markers

Renal superoxide dismutase (SOD)

The superoxide dismutase activity was assessed by colorimetry and a UV spectrophotometer [17]. This process is based on the formation of pyrogallol-quinone through the sod, a reactive intermediate, and the ability of the semiquinone radical to suppress this reaction by radical dismutation. This brown material absorbs visible light at wavelengths below 420 nm.

Renal malondialdehyde (MDA)

This process is merely being offered as a guide. The product manual could differ somewhat. The product manual that was packaged and sent with the item should be followed before using it. Add 50 µl of the standard or sample to each well, followed by 50 µl of the working solution for the biotinylated detection antibody. Aspirate and rinse the plate three times. Include a 100 µL solution of the HRP conjugate. Include 90 µL of the substrate agent. Include 50 µL Stop Solution. Immediately begin reading the plate at 450nm.

Histopathological study

The kidney tissues were treated using standard histological techniques and fixed in paraffin blocks after being fixed in 10% formalin. Hematoxylin-eosin (H&E) was used to stain 5-m thick slices for further histological analysis [18]. An investigator blind to the experimental treatment groups evaluated the scores after fixation. The histopathological damage was evaluated using the following morphological parameters in accordance with the methodology [19].

Score 0: normal.

Score 1: Damaged area< 25% of tubules.

Score 2: Injuries affect 25–50% of the tubules.

Score 3: Damage affecting 50% to 75% of the tubules.

Score 4: 75–100% of the region is affected.

The term "tubular injury" was used to describe tubular epithelial enlargement, loss of brush boundary, capillary degeneration, tubular necrosis, cast formation, and desquamation.

Statistical analysis

The statistical analysis application SPSS 26 was employed. The analysis of variance (ANOVA) with LSD post-hoc test was used to examine group differences. The Kruskal-Wallis with Mann-Whitney U-test was used to examine histological

differences. The statistical determination of the existing data's significance was $p < 0.05$.

Results and Discussion

Impacts of cilostazol on tissue and serum ngal levels

For more documented evident results, both renal and serum levels of the specific renal injury marker NGAL 24 hours after polymicrobial sepsis induced by CLP, all experimental groups were carried out with ELISA assay protocol. ELISA outcomes demonstrated that the serum and tissue levels of NGAL were considerably higher ($p < 0.05$) in the CLP and DMSO groups compared to the apparently healthy group. While the cilostazol group exhibited considerably lower levels ($p < 0.05$) of NGAL if compared with the CLP group. These results agreed with the previous work done by [20], who discovered serum NGAL was significantly higher in septic individuals with AKI than in those without AKI as a function of the severity of the sepsis. NGAL was considered the 'troponin' of the kidney [21] (Figure 1).

Cilostazol leveled off NGAL, reducing renal injury intensity, reducing injured nephrons, and enhancing renal function [22].

Cilostazol's Impacts on Inflammatory Cytokines Levels

To find out the impact of cilostazol on the inflammatory response that occurs during CLP-induced polymicrobial sepsis, the serum levels of inflammatory cytokines, including (IL-1β, TNF-α, and IL-6) were evaluated using the ELISA approach 24 hours after CLP-induced polymicrobial sepsis (Figure 2). The current investigation found that the serum level of inflammatory cytokines (IL-1β, TNF-α, and IL-6) was significantly higher ($p < 0.05$) in the CLP group as compared with the normal group. While the cilostazol group showed markedly lower ($p < 0.05$) levels of inflammatory cytokines (IL-6, TNF-α, and IL-1β) if compared with the CLP group, these findings were consistent with previous studies [23-25]. The rat brain I/R-induced rise in TNF-α is inhibited by cilostazol, which may be strongly linked to elevated cyclic AMP levels. In this investigation, soluble TNF- was elevated during retinal I/R, and cilostazol prevented this elevation. Cilostazol may prevent retinal cell damage and the rise in vascular permeability brought on by retinal I/R by inhibiting the production of TNF-α [26].

Effects of cilostazol oxidative stress biomarker

Cilostazol affects the renal tissue SOD activity (U/mL) in the experimental groups.

The current study outcomes showed that the degree of renal tissue SOD activity was considerably lower ($p < 0.05$) in the CLP and DMSO groups compared to the normal group (Figure 3).

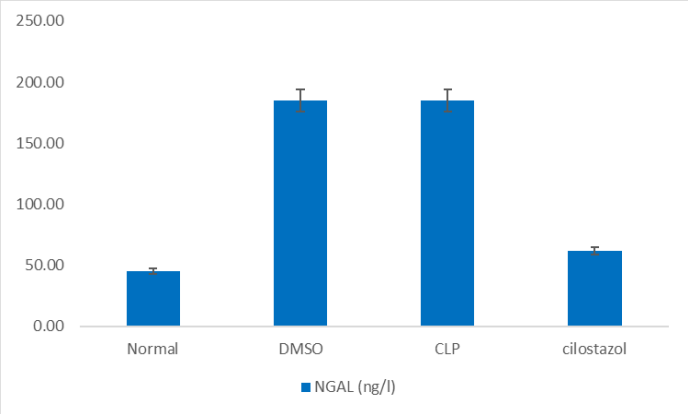

Figure 1: Mean tissue level of NGAL (ng/l) in the experimental groups. *P: significant difference ($p< 0.05$) when compared with the apparently healthy group; #P: significant difference ($p< 0.05$) when compared with the CLP group

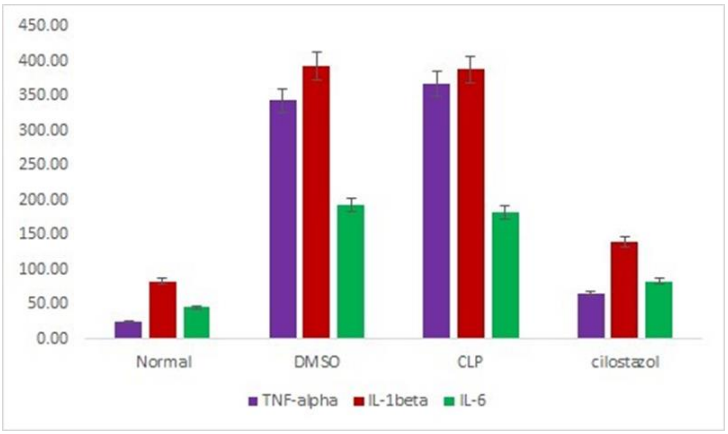

Figure 2: Mean serum level of inflammatory cytokines (IL-1β, TNF-α, and IL-6): Data are expressed as mean ± SD; *P <0.05 versus the normal group; #P <0.05 versus the CLP group

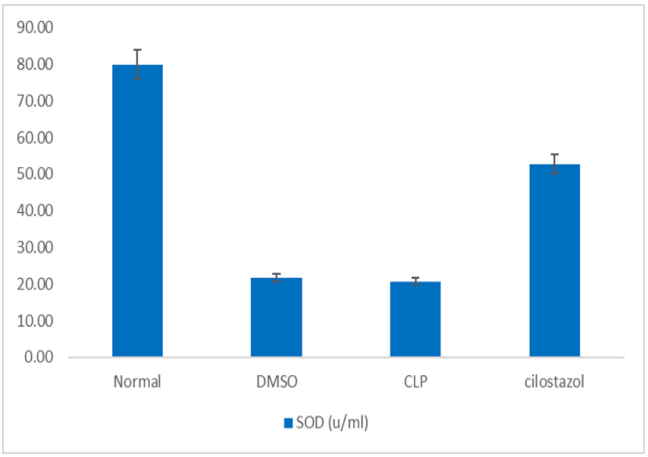

Figure 3: Mean tissue level of SOD activity (U/ml): Data are expressed as mean ± SD; *P <0.05 versus the normal group; #P <0.05 versus the septic group

In contrast, the cilostazol group exhibited a considerably higher degree (p <0.05) of SOD activity than the untreated septic group. Cilostazol inhibited lipid peroxide formation and countered the redox tissue imbalance, perhaps through its capacity to scavenge free radicals or enhance the action of endogenous antioxidants (CAT and SOD) [27].

Effects of cilostazol on the renal tissue level of MDA in the experimental groups

According to the results of the current investigation, the levels of renal tissue MDA were considerably higher (p< 0.05) in the septic and DMSO groups compared to the group that appeared to be in good condition (Figure 4). The MDA levels in the cilostazol group, in contrast to the CLP group, were considerably lower (p< 0.05). According to studies, cilostazol increases the effects of reno-protection against acute renal damage. The primary mechanisms underlying the beneficial effects of antioxidants and drug therapy may involve activation of the endogenous adaptive reno-protective, gene renal nuclear factor erythroid 2-related factor 2Nrf2 and its NADPH-quinone, The calcium sensitizer cilostazol is known for its capacity to neutralize reactive oxygen species (ROS) [28]. Besides its capability to lessen the synthesis of apoptotic proteins and inflammatory cytokines [29, 30].

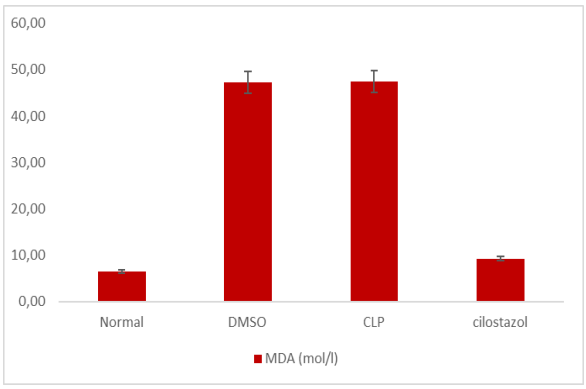

Figure 4: Mean tissue level of MDA activity (mol/l): Data are expressed as mean ± SD; *P <0.05 versus the healthy group; #P <0.05 versus the CLP group

The effect of the cilostazol on histopathological on modifications caused by sepsis

A histological analysis of renal tissue was carried out to further demonstrate the effects of cilostazol. On the renal injury that occurs during polymicrobial sepsis. Following 24 hours of CLP-induced polymicrobial sepsis, serial renal tissue slices were taken for this histological investigation and staining with hematoxylin and eosin (H&E). Following is a summary of the histopathology results for each group of mice. CLP renal tissue demonstrated significant ($P < 0.05$) renal damage compared to the apparently healthy group, showing degenerated renal tubules. Hemorrhage in the interstitial tissue enlarged sub-capsular space and glomerular tuft degeneration and necrosis of the epithelial cells in the renal tubules. This group had 10% mild, 50% moderate, and 40% severe histological grading from normal renal tissue, and the final score was severe. While the cilostazol group showed a considerable ($P<0.05$) reduction in renal injury compared to the CLP group. Cilostazol group histological changes arranged from mild to moderate changes. As shown in Figures 5, 6, and 7. Regarding histopathological grading from normal renal tissue, the cilostazol group showed 60% mild and 40% moderate and the final score was mild damage. During sepsis-induced renal damage there were several histological alterations have been observed during sepsis-induced kidney injury, including the CLP procedure caused significant induced kidney injury in rats by inducing sepsis because the CLP group displayed increased inflammatory infiltration, obvious edema, significant hemorrhagic spots in the interstitium, narrower renal tubules, enlarged glomerular, and degenerated epithelial cells [31]. The mice in the apparently healthy group showed normal architecture without neutrophil infiltration and normal glomerulus and renal tubules; comparing the CLP group to the apparently healthy group in the current investigation, a significant histopathological alteration was seen in the CLP group. Showing degenerated renal tubules, hemorrhage in the interstitial tissue enlarged sub-capsular space, and glomerular tuft degeneration and necrosis of the epithelial cells in the renal tubules, these findings are consistent with a previous study that was done on mice to investigate how sirtuin 3 prevents sepsis-induced acute kidney damage in a mouse model [32]. Additionally, in the current study, the cilostazol group showed a significantly reduced level of renal tissue injury. Compared with the CLP group, the cilostazol group showed mild to moderate changes including renal tubule dilation, a necrotic nucleus with the deformed architecture of renal tubules with hemorrhage, and glomerulonephritis. These findings agreed with a previous study that studied the effect of cilostazol on gentamicin-induced nephrotoxicity in rats [33]. These protective effects of cilostazol on the renal tissue that resulted from the pre-treatment with cilostazol can be attributed to its mechanisms of action as the anti-inflammatory and antioxidant agent, which counteract the pathological effect on the renal that occurs during polymicrobial sepsis induced by the CLP model [34].

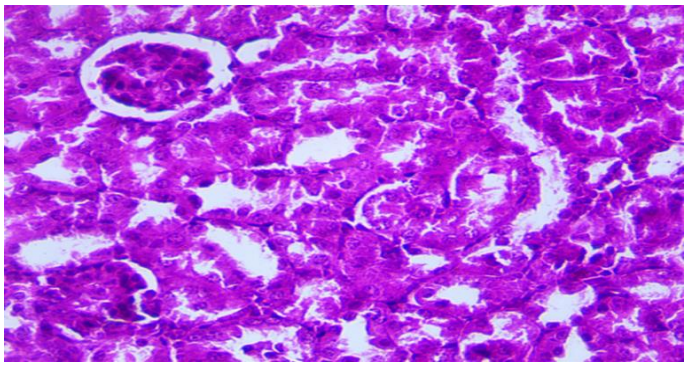

Figure 5: Cross section of the kidney of mice in the healthy group shows normal all architecture of tissue (40x), (H & E). Orange arrows show normal glomeruli; black arrows show normal renal tubules and no neutrophil infiltration

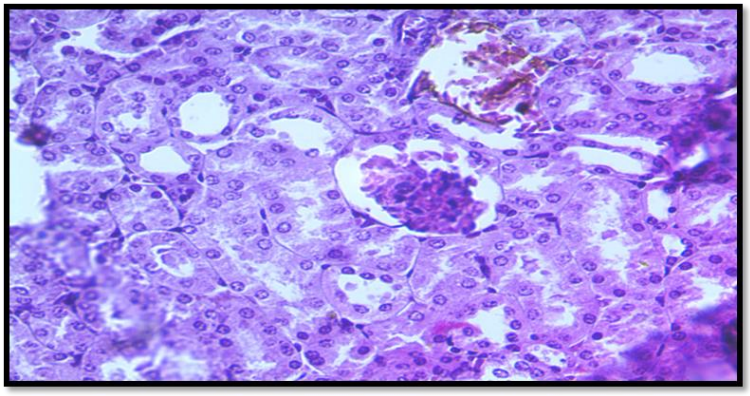

Figure 6: Cross section of the renal mice, CLP, (A) showed degenerated renal tubules (1) (B) hemorrhage in the interstitial tissue (2) enlarged sub-capsular space and glomerular tuft degeneration (3) and the arrows indicate necrosis of the epithelial cells in the renal tubules. (H and E) (10X&40X)

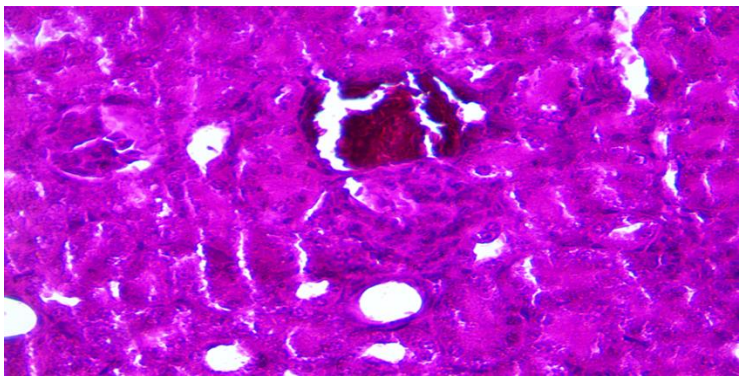

Figure 7: Cross section of the kidney mice cilostazol group, the black arrow show renal tubule dilation orange arrow show necrotic nucleus with the deformed architecture of renal tubules with hemorrhage, and the green arrow show glomerulonephritis. (E&H)(40X)

Conclusion

Cilostazol demonstrates itś renoprotective effects, possibly through itś anti-inflammatory and antioxidant effects. Cilostazol also exhibits renoprotective properties by suppressing the expression of a renal-specific marker (NGAL). In addition, these medications have a nephroprotective impact by reducing the histological alterations that result from polymicrobial sepsis.

Funding

This research did not receive any specific grant from funding agencies in the public, commercial, or not-for-profit sectors.

Authors' contributions

All authors contributed to data analysis, drafting, and revising of the paper and agreed to be responsible for all the aspects of this work.

Conflict of Interest

The author declared that they have no conflict of interest.

ORCID:

Abdulla K Raheem
https://orcid.org/0000-0001-8181-3879
Qassim A Zigam
https://orcid.org/0000-0002-1425-3450

References

[1]. Vincent J.L., Marshall J.C., Ñamendys-Silva S.A., François B., Martin-Loeches I., Lipman J., Reinhart K., Antonelli M., Pickkers P., Njimi H., Jimenez E., Sakr Y., Assessment of the worldwide burden of critical illness: the intensive care over nations (ICON) audit, *The lancet Respiratory medicine*, 2014, **2**:380 [Crossref], [Google Scholar], [Publisher]

[2]. Seymour C.W., Liu V.X., Iwashyna T.J., Brunkhorst F.M., Rea T.D., Scherag A., Rubenfeld G., Kahn J.M., Shankar-Hari M., Singer M., Deutschman C.S., Escobar G.J., Angus D.C., Assessment of clinical criteria for sepsis: for the Third International Consensus Definitions for Sepsis and Septic Shock (Sepsis-3), *Jama*, 2016, **315**:762 [Crossref], [Google Scholar], [Publisher]

[3]. Askari Y., Mohtashami R., Evaluation of Thymus Vulgaris, Salvia Officinalis, Mentha Piperita and Hyssopus Officinalis Plants with Benefits on the Respiratory Organs, *International Journal of Advanced Biological and Biomedical Research*, 2022, **10**:173 [Crossref], [Google Scholar], [Publisher]

[4]. Hoste E.A., Bagshaw S.M., Bellomo R., Cely C.M., Colman R., Cruz D.N., Edipidis K., Forni L.G., Gomersall C.D., Govil D., Honoré P.M., Joannes-Boyau O., Joannidis M., Korhonen A.M., Lavrentieva A., Mehta R.L., Palevsky P., Roessler E., Ronco C., Uchino S., Vazquez J.A., Andrade E.V., Webb S., Kellum J.A., Epidemiology of acute kidney injury in critically ill patients: the multinational AKI-EPI study, *Intensive care medicine*, 2015, **41**:1411 [Crossref], [Google Scholar], [Publisher]

[5]. Maiden M.J., Otto S., Brealey J.K., Finnis M.E., Chapman M.J., Kuchel T.R., Nash C.H., Edwards J., Bellomo R., Structure and function of the kidney in septic shock. A prospective controlled experimental study, *American journal of respiratory and critical care medicine*, 2016, **194**:692 [Crossref], [Google Scholar], [Publisher]

[6]. Rogers K.C., Oliphant C.S., Finks S.W., Clinical efficacy and safety of cilostazol: a critical review of the literature, *Drugs*, 2015, **75**:377 [Crossref], [Google Scholar], [Publisher]

[7]. Hasanpour F., Taei M., Fouladgar M., Salehi M., 'Au nano dendrites/composition optimized Nd-dopped cobalt oxide as an efficient electrocatalyst for ethanol oxidation', *Journal of Applied Organometallic Chemistry*, 2022, **2**:203 [Crossref], [Google Scholar], [Publisher]

[8]. Bangalore S., Singh A., Toklu B., DiNicolantonio J.J., Croce K., Feit F., Bhatt D.L., Efficacy of cilostazol on platelet reactivity and cardiovascular outcomes in patients undergoing percutaneous coronary intervention: insights from a meta-analysis of randomised trials, *Open Heart*, 2014, **1**:e000068 [Crossref], [Google Scholar], [Publisher]

[9]. Jinno J.I., Kamada N., Miyake M., Yamada K., Mukai T., Odomi M., Toguchi H., Liversidge G.G., Higaki K., Kimura T., Effect of particle size reduction on dissolution and oral absorption of a poorly water-soluble drug, cilostazol, in beagle dogs, *Journal of Controlled Release*, 2006, **111**:56 [Crossref], [Google Scholar], [Publisher]

[10]. John B., Habila J., Oyewale A., Tukur A., 'Isolation, Characterization and Antimalarial Evaluation of Methyl-3,12-dihydroxycholan-24-oate from Bovine Bile', *Advanced Journal of Chemistry-Section B: Natural Products and Medical Chemistry*, 2022, **4**:135 [Crossref], [Google Scholar], [Publisher]

[11]. Reddy, S.S., Agarwal H., Barthwal M.K., Cilostazol ameliorates heart failure with preserved ejection fraction and diastolic dysfunction in obese and non-obese hypertensive mice, *Journal of molecular and cellular cardiology*,

2018, **123**:46 [Crossref], [Google Scholar], [Publisher]
[12]. Wen H., Sepsis induced by cecal ligation and puncture, In *Mouse Models of Innate Immunity*, Humana Press, Totowa, NJ, 2013, **1031**:117 [Crossref], [Google Scholar], [Publisher]
[13]. Budi H.S., Elveny M., Zhuravlev P., Jalil A.T., Al-Janabi S., Alkaim A.F., Saleh M.M., Shichiyakh R.A., Development of an adaptive genetic algorithm to optimize the problem of unequal facility location, *Foundations of Computing and Decision Sciences*, 2022, **47**:111 [Crossref], [Google Scholar], [Publisher].
[14]. Coldewey S.M., Rogazzo M., Collino M., Patel N.S., Thiemermann C., Inhibition of IκB kinase reduces the multiple organ dysfunction caused by sepsis in the mouse, *Disease models & mechanisms*, 2013, **6**:1031 [Crossref], [Google Scholar], [Publisher]
[15]. Zhang J., Cheng X., Liao Y.H., Lu B., Yang Y., Li B., Guo Z., Zhang L., Simvastatin regulates myocardial cytokine expression and improves ventricular remodeling in rats after acute myocardial infarction, *Cardiovascular drugs and therapy*, 2005, **19**:13 [Crossref], [Google Scholar], [Publisher]
[16]. Ali M., Opulencia M.J.C., Chandra T., Chandra S., Muda I., Dias R., Chetthamrongchai P., Jalil A.T., An Environmentally Friendly Solution for Waste Facial Masks Recycled in Construction Materials, *Sustainability*, 2022, **14**:8739 [Crossref], [Google Scholar], [Publisher]
[17]. Marklund S., Marklund G., Involvement of the superoxide anion radical in the autoxidation of pyrogallol and a convenient assay for superoxide dismutase, *European journal of biochemistry*, 1974, **47**:469 [Crossref], [Google Scholar], [Publisher]
[18]. Suvarna K.S., Layton C., Bancroft J.D., *Bancroft's theory and practice of histological techniques E-Book*, Elsevier health sciences, 2018 [Google Scholar], [Publisher]
[19]. Raya I., Danshina S., Jalil A.T., Suksatan W., Mahmoud M.Z., Roomi A.B., Mustafa Y.F., Kazemnejadi M., Catalytic filtration: efficient CC cross-coupling using Pd (II)-salen complex-embedded cellulose filter paper as a portable catalyst, *RSC advances*, 2022, **12**:20156 [Crossref], [Google Scholar], [Publisher]
[20]. Wang M., Zhang Q., Zhao X., Dong G., Li C., Diagnostic and prognostic value of neutrophil gelatinase-associated lipocalin, matrix metalloproteinase-9, and tissue inhibitor of matrix metalloproteinases-1 for sepsis in the Emergency Department: an observational study, *Critical Care*, 2014, **18**:634 [Crossref], [Google Scholar], [Publisher]
[21]. Schmidt-Ott K.M., Mori K., Li J.Y., Kalandadze A., Cohen D.J., Devarajan P., Barasch J., Dual action of neutrophil gelatinase–associated lipocalin, *Journal of the American Society of Nephrology*, 2007, **18**:407 [Crossref], [Google Scholar], [Publisher]
[22]. Ragab D., Abdallah D.M., El-Abhar H.S., Cilostazol renoprotective effect: modulation of PPAR-γ, NGAL, KIM-1 and IL-18 underlies its novel effect in a model of ischemia-reperfusion, *PLoS One*, 2014, **9**:e95313 [Crossref], [Google Scholar], [Publisher]
[23]. Sivaraman R., Patra I., Opulencia M.J.C., Sagban R., Sharma H., Jalil A.T., Ebadi A.G., Evaluating the potential of graphene-like boron nitride as a promising cathode for Mg-ion batteries, *Journal of Electroanalytical Chemistry*, 2022, **917**:116413 [Crossref], [Google Scholar], [Publisher]
[24]. An Y., Zheng Z., Zhang X., Cho S.B., Kim D.Y., Choi M.J., Bang D., Cilostazol inhibits the expression of hnRNP A2/B1 and cytokines in human dermal microvascular endothelial cells, *Clinical and experimental rheumatology*, 2017, **35**:S60 [Google Scholar]
[25]. El-Abhar H., Abd El Fattah M.A., Wadie W., El-Tanbouly D.M., Cilostazol disrupts TLR-4, Akt/GSK-3β/CREB, and IL-6/JAK-2/STAT-3/SOCS-3 crosstalk in a rat model of Huntington's disease, *Plos one*, 2018, **13**:e0203837 [Crossref], [Google Scholar], [Publisher]
[26]. Ishizuka F., Shimazawa M., Egashira Y., Ogishima H., Nakamura S., Tsuruma K., Hara H., Cilostazol prevents retinal ischemic damage partly via inhibition of tumor necrosis factor-α-induced nuclear factor-kappa B/activator protein-1 signaling pathway,

Pharmacology Research & Perspectives, 2013, **1** [Crossref], [Google Scholar], [Publisher]

[27]. Fitriyah A., Nikolenko D.A., Abdelbasset W.K., Maashi M.S., Jalil A.T., Yasin G., Abdulkadhm M.M., Samieva G.U., Lafta H.A., Abed A.M., Amaral L.S., Mustafa Y.F., Exposure to ambient air pollution and osteoarthritis; an animal study, *Chemosphere*, 2022, **301**:134698 [Crossref], [Google Scholar], [Publisher]

[28]. Gokce M., Yuzbasioglu M.F., Bulbuloglu E.R.T.A.N., Oksuz H., Yormaz S., Altınoren O., Kutlucan M., Coskuner I., Kale I.T., Cilostazol and diltiazem attenuate cyclosporine-induced nephrotoxicity in rats, In *Transplantation proceedings*, Elsevier, 2012, **44**:1738 [Crossref], [Google Scholar], [Publisher]

[29]. Lee J.H., Oh G.T., Park S.Y., Choi J.H., Park J.G., Kim C.D., Lee W.S., Rhim B.Y., Shin Y.W., Hong K.W., Cilostazol reduces atherosclerosis by inhibition of superoxide and tumor necrosis factor-α formation in low-density lipoprotein receptor-null mice fed high cholesterol, *Journal of Pharmacology and Experimental Therapeutics*, 2005, **313**:502 [Crossref], [Google Scholar], [Publisher]

[30]. Tawfik M.K., Makary S., Keshawy M.M., Upregulation of antioxidant nuclear factor erythroid 2-related factor 2 and its dependent genes associated with enhancing renal ischemic preconditioning renoprotection using levosimendan and cilostazol in an ischemia/reperfusion rat model, *Archives of Medical Science: AMS*, 2021, **17**:1783 [Crossref], [Google Scholar], [Publisher]

[31]. Gunawan W., Rudiansyah M., Sultan M.Q., Ansari M.J., Izzat S.E., Al Jaber M.S., Kzar H.H., Mustafa Y.F., Hammid A.T., Jalil A.T., Aravindhan S., Effect of tomato consumption on inflammatory markers in health and disease status: A systematic review and meta-analysis of clinical trials, *Clinical Nutrition ESPEN*, 2022, **50**:93 [Crossref], [Google Scholar], [Publisher]

[32]. Salahdin O.D., Sayadi H., Solanki R., Parra R.M.R., Al-Thamir M., Jalil A.T., Izzat S.E., Hammid A.T., Arenas L.A.B., Kianfar E., Graphene and carbon structures and nanomaterials for energy storage, *Applied Physics A*, 2022, **128**:703 [Crossref], [Google Scholar], [Publisher]

[33]. Abdelsameea A.A., Mohamed A.M., Amer M.G., Attia S.M., Cilostazol attenuates gentamicin-induced nephrotoxicity in rats, *Experimental and Toxicologic Pathology*, 2016, **68**:247 [Crossref], [Google Scholar], [Publisher]

[34]. Hafez H.M., Ibrahim M.A., Zedan M.Z., Hassan M., Hassanein H., Nephroprotective effect of cilostazol and verapamil against thioacetamide-induced toxicity in rats may involve Nrf2/HO-1/NQO-1 signaling pathway, *Toxicology Mechanisms and Methods*, 2019, **29**:146 [Crossref], [Google Scholar], [Publisher]

HOW TO CITE THIS ARTICLE

Abdulla K Raheema, Ahmed R. Abu-Raghif, Qassim A Zigam. Cilostazol protects against sepsis-induced kidney impairment in a mice model. *J. Med. Chem. Sci*., 2023, 6(5) 1193-1203

https://doi.org/10.26655/JMCHEMSCI.2023.5.25

URL: http://www.jmchemsci.com/article_160164.html